SCIENTIFIC PAPER
Published: December 30, 2024
https://doi.org/10.13167/2024.29.9

Evaluation of mechanical properties of sustainable and eco-friendly ultra-high-performance concrete using ternary cementitious binders

Vineet Kothari[1] and Urmil Dave[1]

[1] Nirma University, Institute of Technology, Civil Engineering Department, Charrodi, S. G. Highway, 382481, Ahmedabad, India

Corresponding author:
Urmil Dave
urmil.dave@nirmauni.ac.in

Received:
February 21, 2024

Revised:
May 6, 2024

Accepted:
July 2, 2024

Published:
December 30, 2024

Citation:
Kothari, V.; Dave, U. Evaluation of mechanical properties of sustainable and eco-friendly ultra-high-performance concrete using ternary cementitious binders. *Advances in Civil and Architectural Engineering,* 2024, 15 (29), pp. 137-150. https://doi.org/10.13167/2024.29.9

ADVANCES IN CIVIL AND ARCHITECTURAL ENGINEERING (ISSN 2975-3848)

Faculty of Civil Engineering and Architecture Osijek
Josip Juraj Strossmayer University of Osijek
Vladimira Preloga 3
31000 Osijek
CROATIA

Abstract:
Building structures using Ultra-High Performance Concrete (UHPC) with better mechanical and durability properties requires effort and consideration for the environment. The present study comprises 17 distinct trial mixes or UHPC. The cementitious content ranges from 1200-1400 kg/m3, the water-to-cementitious ratio varies from 0,16-0,18, and micro-steel fibres measuring 0,2 × 13,0 mm are included at a proportion of 1,5 % of the total concrete volume. A variety of ingredients including cement, fly ash, micro-silica, fine sand, high-range water reducer, shrinkage reducing admixture, micro-steel fibres and water were utilised. Specimens were cast and evaluated at 7, 14, and 28 days for mechanical properties such as flexural, indirect tensile, and compressive strength, as well as fresh concrete characteristics, such as the slump cone test. The results indicate that there was an improvement in the slump cone value as the fly ash content increased. The mechanical characteristics were enhanced by the increase in micro-silica, which is attributed to the refining of the pore structure and the pozzolanic reactivity during the early stages. Optimal blend ratio for maximizing the compressive, tensile and flexural strength of UHPC has been identified in mixes where 15-20 % of cement has been replaced by Supplementary Cementitious Materials (SCMs) in various combinations. The replacement ratio was found to enhanced mechanical properties due to optimized particle packing and improved matrix density within the concrete.

Keywords:
ultra-high-performance concrete (UHPC); water-to-binder ratio; indirect tensile strength; compressive strength; flexural strength; micro-streel fibres

1 Introduction

Concrete is commonly employed in construction because of its exceptional strength and durability. Ultra-high-performance concrete (UHPC) exhibits a water-to-cementitious ratio (w/c) < 0,25 and is devoid of any microscopic imperfections. The inclusion of a higher amount of steel fibres in this material resulted in compressive strength greater than 120 MPa and tensile strength greater than 6 MPa [1]. UHPC reinforced with fibres exhibits a low ratio of water to cementitious materials. It utilises more refined granular sand in place of the aggregate to achieve enhanced performance. By optimising the granular structure of the concrete, its strength can be increased to 280 MPa [2]. Traditional UHPC comprises cement, steel fibres, quartz sand, a high-range water reducer, and silica fume [3].

Before the 1980s, vacuum mixing and high temperatures boosted the strength, but they were difficult and energy-intensive [4]. Polymers were used to plug concrete pores and produce defect-free concrete in the early 1980s [5]. The term UHPC arose in the 1990s alongside reactive powder concrete (RPC), which has many uses. The brittleness, high-upfront costs, complicated methods, and limited laboratory-scale manufacturing of UHPC render its mass production difficult [6]. RPC became popular in the 2000s owing to its extensive manufacturing. Subsequently, Canada built its first pedestrian bridge [7].

UHPC uses two to three times more cement than ordinary concrete. Increased infrastructural development and towering building use are to blame for these developments; therefore, sustainable UHPC is essential. The uses of fly ash, GGBS, silica fume, rice husk ash, and metakaolin have been investigated for sustainable UHPC use [8-14]. The Supplementary Cementitious Materials (SCMs) used in UHPC determine their packing densities. At increasing micro-structural densities, the mechanical properties and durability qualities of UHPC improved [15, 16]. Traditional UHPC types are mostly composed of cement, silica fume, quartz powder, steel fibres, and a high-range water reducer. However, researchers have shown growing interest in the use of SCMs to produce sustainable UHPC.

The application of various SCMs in commercial UHPC development is restricted by their uneven material characteristics [17-19]. Traditional materials are combined into ternary and quaternary mixes. Dilution from increasing GGBS and fly ash dosage decreased the potency at a later age [20]. Owing to the increase in temperature, curing led to a decrease in fluidity and an increase in the mechanical properties [21]. A higher packing density can also improve the overall properties of UHPC in the ternary and quaternary mixes [22]. Utilising fly ash cenospheres can enhance fluidity but may lead to a reduction in the overall strength of UHPC [23].

The incorporation of ultra-fine fly ash in combination with steel fibres has shown the potential to enhance the post-cracking behaviour of UHPC [24]. Various materials, such as fly ash, slag, rice husk ash, and metakaolin, have been explored as partial replacements for micro-silica [25, 26]. UHPC was subjected to tests involving higher levels of replacement and was examined for its mechanical and durability properties [27, 28]. The partial replacement of fly ash with TiO2 was observed to increase the overall strength of UHPC [29]. Furthermore, the increase in fly ash and slag content typically enhances the overall flow but diminishes at higher silica fume contents. However, there is a dearth of evidence concerning the optimal ingredient combinations and dosages required to advance UHPC technology.

According to the literature, UHPC should be developed using local materials. Supplementary Cementitious Materials (SCMs) are pozzolanic industrial waste. These compounds improve the mechanical strength and durability of concrete. This study utilised fly ash (10-25 %) and micro-silica (10-25 %) to assess the sustainability and environmental friendliness of UHPC combinations. The compressive, indirect tensile, and flexural strengths of the mixes were measured and compared.

2 Experimental Programme

2.1 Raw materials

In this study, OPC cement (53 grade) (IS12269-1987) [30], micro silica, fly ash, micro-steel fibres, a high-range water reducer (HRWR), shrinkage-reducing admixture (SRA), and water were employed to develop UHPC. Table 1 lists the chemical and physical parameters of the raw materials used in the study. UHPC used 2 mm fine sand as a fine aggregate. The specific gravity of the fine sand was 2,67 and its bulk density was 1780 kg/m^3. The HRWR and SRA were used at the rates of 1,5 % and 1,0 % of the total cementitious material, respectively. Brass-coated micro-steel fibres with a length of 13 mm length, diameter of 0,2 mm, and a tensile strength of 2350 MPa were used. Table 2 lists the characteristics of the steel fibres. The experimental setup is illustrated in Figure 1.

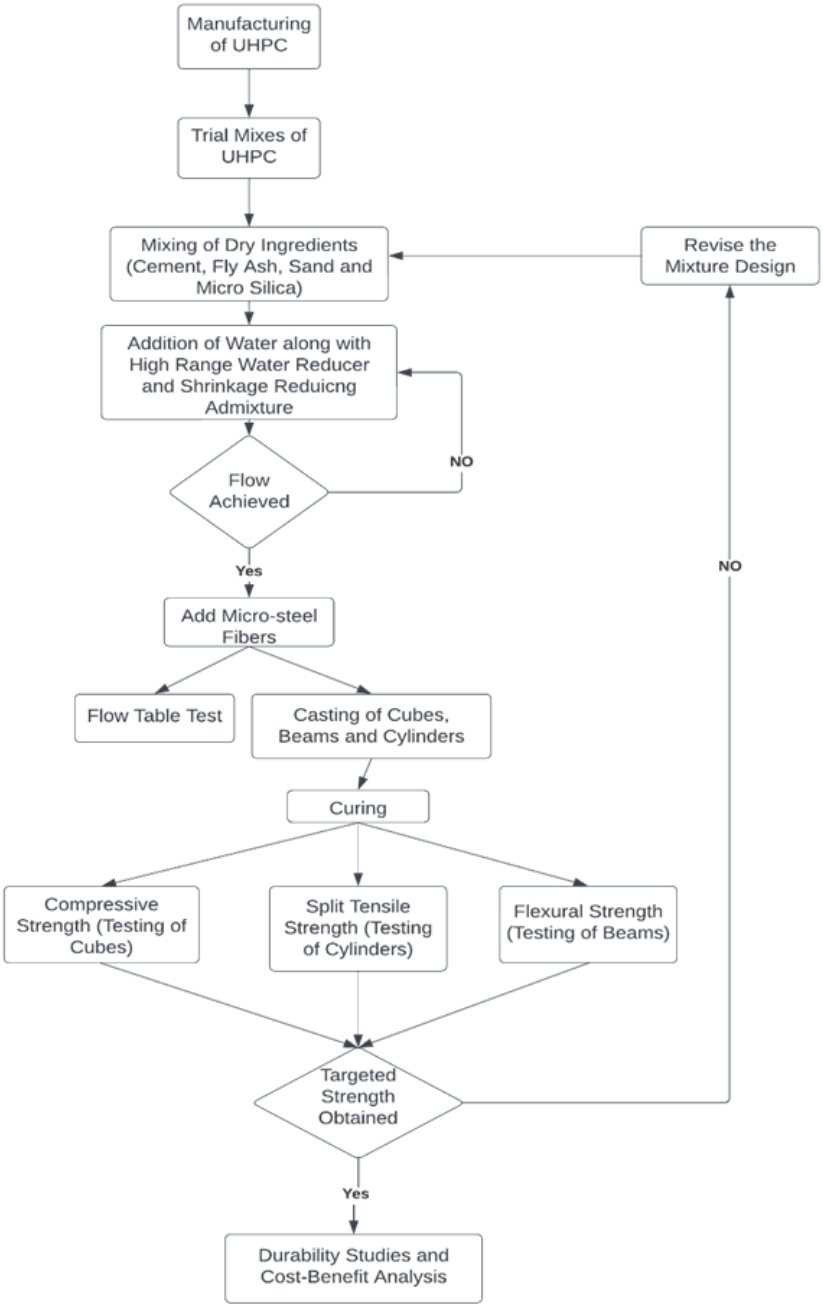

Figure 1. Experimental programme

Table 1. Physical and chemical properties of materials

Chemical and physical properties (oxides, % by weight)	OPC	MicroSilica	Fly Ash
SiO_2	18,10	95,00	45,50
CaO	62,10	0,42	5,00
Fe_2O_3	2,20	0,23	4,00
SO_3	2,62	0,52	1,10
Al_2O_3	5,20	0,61	31,10
K_2O	1,30	0,14	0,14
MgO	4,10	0,22	1,20
Na_2O	0,35	0,21	0,21
loss on ignition	2,50	2,10	2,10
Blaine fineness (m^2/kg)	303,00	22000,00	410,00
specific gravity	3,20	2,21	2,26

Table 2. Properties of Steel Fibres

Physical properties	Value
Density	7850 kg/m^3
Diameter	0,22 mm
Length	13 mm
Mechanical properties	**Value**
Tensile Strength	2350 kg/m^3
Modulus of Elasticity	GPa

2.2 Mixture design proportions

Seventeen mixes were considered to determine the optimum dosages of cement, micro silica, and fly ash, as listed in Table 3. Mix 0 was considered a control mix without fly ash. Mixes 1-8 and 9-16 were considered to have cementitious contents of 1200 kg/m^3 and 1400 kg/m^3, respectively. The mixture design was considered based on the recommendations given by Azmee et al. [4]. In conventional UHPC formulations, a substantial part of cement, micro silica, quartz powder, high-range water reducer, and shrinkage-reducing admixture was combined with steel fibres. The cementitious content typically ranges from 1200 to 1400 kg/m^3. Additionally, the binder-to-sand ratio was maintained within the range of 1,1-1,5.
For all mixes, the HRWR, SRA, and steel fibres remained constant throughout all the mixes. Considering weight-based batching for the UHPC cement content varies from 60-75 %, fly ash varies from 10-25 %, and micro-silica varies from 10-25 % of the total cementitious content. According to the ASTM C1856 standard, the targeted flow for the various mixes was at a minimum of 200 mm [31]. The Water-to-Binder (W/B) ratio remained constant at 0.18 for Mixes 0-8 and was 0,16 for Mixes 9-16 to adhere to the requirements of flow according to the modified flow table test given in the ASTM C1856 standard. The binder-to-fines ratio remained at 1,0 for Mixes 0–8 and was equal to 1,5 for Mixes 9-16. The mix designations represent combinations of existing binders with different replacements. For example, Mix 1 represents the mix designations as C-60/F-20/M-15, where cement constitutes 60% of the total binder content, while fly ash and micro-silica make up 20 % and 15 %, respectively. The mixture design details are shown in Tables 3 and 4.

Table 3. Mixture design details for Mixes 0-8

Material (kg/m^3)	Mix 0 C-85/M-15	Mix 1 C-60/F-25/M-15	Mix 2 C-65/F-20/M-15	Mix 3 C-60/F-20/M-20	Mix4 C-65/F-10/M-25	Mix 5 C-70/F-15/M-15	Mix 6 C-70/F-10/ M-15	Mix 7 C-70/F-10 M-20	Mix 8 C-75/F-15/M-10
cement	1028,0	725,0	786,0	725,0	786,0	847,0	907,5	847,0	907,5
fly ash	-	303,0	242,0	242,0	121,0	181,5	121,0	121,0	181,5
micro silica	182,0	182,0	182,0	242,0	303,0	181,5	181,5	242,0	121,0
fine sand	1119,00								
steel fibres (0,2 × 12,0 mm)	118,00								
high range water reducer	18,15								
shrinkage reducing admixture	12,10								
water	218,00								
w/b ratio	0,18								
c/a ratio	0,92	0,65	0,70	0,65	0,70	0,76	0,81	0,76	0,81

Table 4. Mixture design details for Mixes 9-16

Material (kg/m^3)	Mix 9 C-60/ F-25/ M-15	Mix 10 C-65/ F-20/ M-15	Mix 11 C-60/ F-20/ M-20	Mix 12 C-65/ F-10/ M-25	Mix 13 C-70/ F-15/ M-15	Mix 14 C-75/ F-10/ M-15	Mix 15 C-70/ F-10/ M-20	Mix 16 C-75/ F-15/ M-10
cement	840	910	840	910	980	1050	980	1050
fly ash	350	280	280	140	210	140	140	210
micro silica	210	210	280	350	210	210	280	140
fine sand	929,00							
steel fibres (0,2 × 12,0 mm)	118,00							
high range water reducer	21,00							
shrinkage reducing admixture	14,00							
water	224,00							
w/b ratio	0,16							
c/a ratio	0,75	0,98	0,90	0,98	1,05	1,13	1,05	1,13

2.3 Specimen preparation, casting, and curing

Seventeen experimental mixes were used in this study. Using a 50 litres of planetary mixer was used to ensure a homogeneous mixture and proper particle dispersion. A specimen measuring 100 × 100 × 100 mm was employed for the compressive strength test, as stated in IS 516 (Part 1):2021[32]. A cylindrical specimen with a diameter of 100 mm and a length of 200 mm was used to test the indirect tensile strength according to the ACI 363 standard. The flexural strength was evaluated using 40 × 40 × 160 mm prisms according to the IS 4031 (Part 8) 1988 [33] requirements. After casting, the curing process was conducted at 25 ± 2 °C, at a relative humidity > 90 %, until testing. Three specimens of each mixture were evaluated for

their flexural and compressive strengths at 7, 14, and 28 d. The indirect tensile strength was measured at the end of 14 and 28 d.

Cube specimens were used to measure the compressive strength of the concrete per IS 516 (Part 1). The experimental setup is shown in Figure 2a (the maximum load was measured, and the compressive strength was calculated using Eq. (1):

$$f_{ck} = \frac{P}{A} \quad (1)$$

The variables f_{ck}, P, and A represent the cross-sectional area, maximum applied load, and compressive strength of the concrete, respectively.

The indirect tensile strength of the concrete was measured using cylindrical specimens with a diameter of 100 mm and height of 200 mm in accordance with the IS 516:2021 standard [23]. Figure 2b shows the experimental configuration. The indirect tensile strength is calculated using Eq. (2):

$$f_{ct} = \frac{2P}{\pi LD} \quad (2)$$

where f_{ct} denotes the indirect tensile strength of the concrete, P is the maximum force applied, L is the length, and D is the diameter of the specimen.

The flexural strength of concrete was evaluated using a three-point bending test, as specified in the IS 4031 standard (Part 8) [24]. The experimental setup is depicted in Figure 2c, where the maximum load was determined and the flexural strength was estimated using the following equation:

$$f_{cf} = \frac{3PL}{2BD^2} \quad (3)$$

The flexural strength is denoted as f_{cf}. The length (mm), width (mm), and depth (mm) of the specimen are denoted by B and D, respectively, and the maximum force applied is denoted by P.

To determine workability, a modified flow table test was performed in accordance with the ASTM C143/143M [34]. A miniature slump cone with a height of 50 mm, top diameter of 70 mm, and a bottom diameter of 100 mm was used. Figure 3a and 3b depict the slump cone and its measurements, respectively.

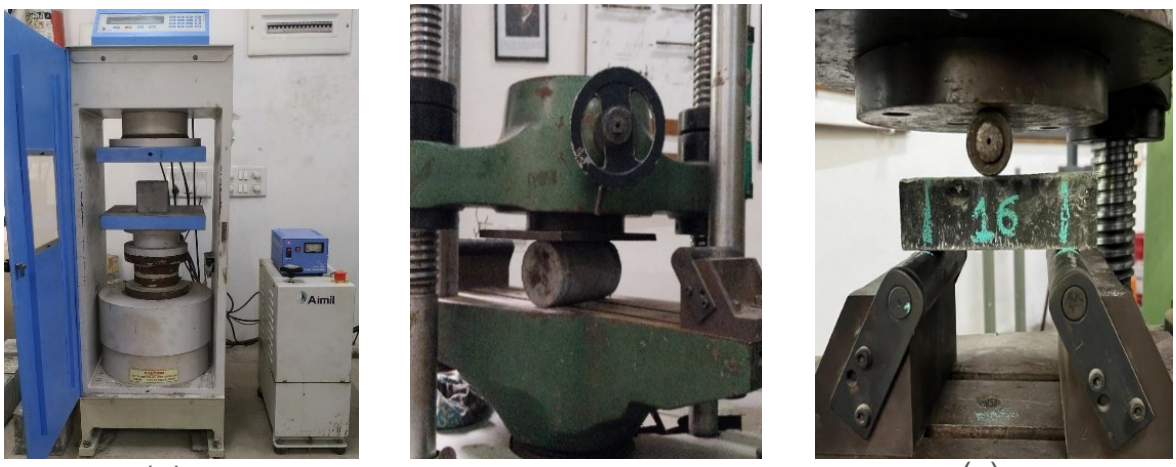

(a) (b) (c)

Figure 2. Test setup for: (a) compressive, (b) indirect tensile, and (c) flexural strength tests

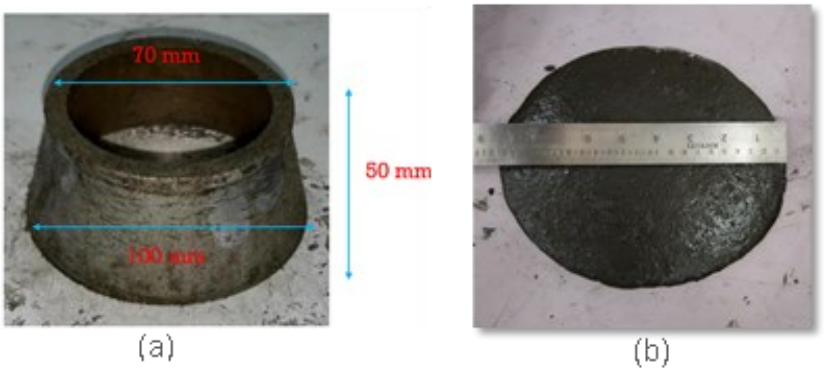

Figure 3. (a) mini slump cone and (b) slump cone measurements

3 Results and discussion

3.1 Workability of UHPC

Figure 4a shows the flow table test flow values for all the mixes. According to the ASTM C1856, the modified flow test for UHPC requires 200 mm. As shown, all the mixes flowed beyond 200 mm. Increasing the amount of micro-silica in the following blends decreased the flow. This is supported by the findings Ge et al. [35], where the flow values of Mixes 9-16 surpassed those of Mixes 0-8. This increase is attributed to the higher binder content achieved at lower water-to-binder ratios.

3.2 Compressive strength of UHPC

Figure 4b shows the compressive strengths for Mixes 0-8 and 9-16. The strength increased gradually from Mix 0-8, with an increase of > 5 % between Mixes 1 and 2 and 2 and 3, for micro-silica contents up to 20 %. The addition of micro-silica did not improve the overall compaction. The C-85/M-15 mixes were stronger than the other fly ash mixes with the same binder content. While replacing cement with fly ash reduces early-age strength, it results in strength gains at later ages. Mixes 5-8 were stronger after 28 d than mixes 1-4. Increased cement content improved the strength by 9-16 d after 28 d. Mixes 13 and 14 exhibited the highest compressive strengths. As reported by Mashaly et al. [36], blends containing 15 % micro-silica combined with fly ash demonstrated superior strength, aligning with our findings. Figure 5 illustrates the relationship between compressive strength and cement-to-aggregate ratio. This demonstrated that increasing the cement content enhanced the overall strength. However, this also underscores the importance of examining the additional impacts of micro-silica and fly ash contents on strength.

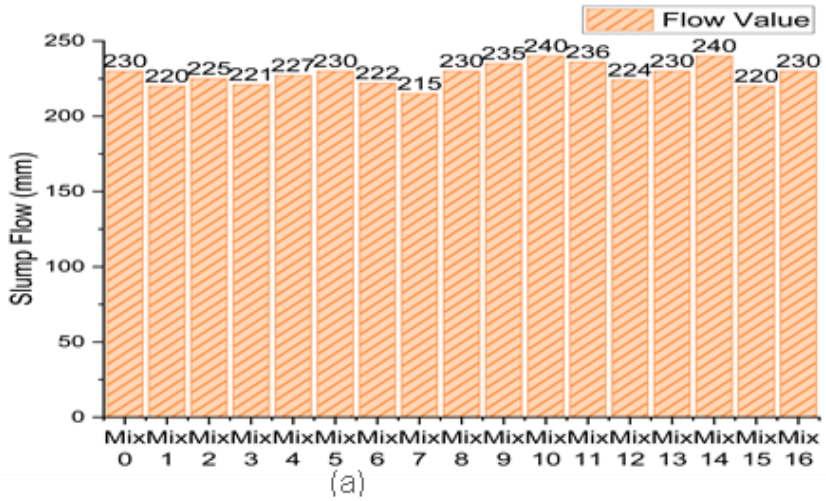

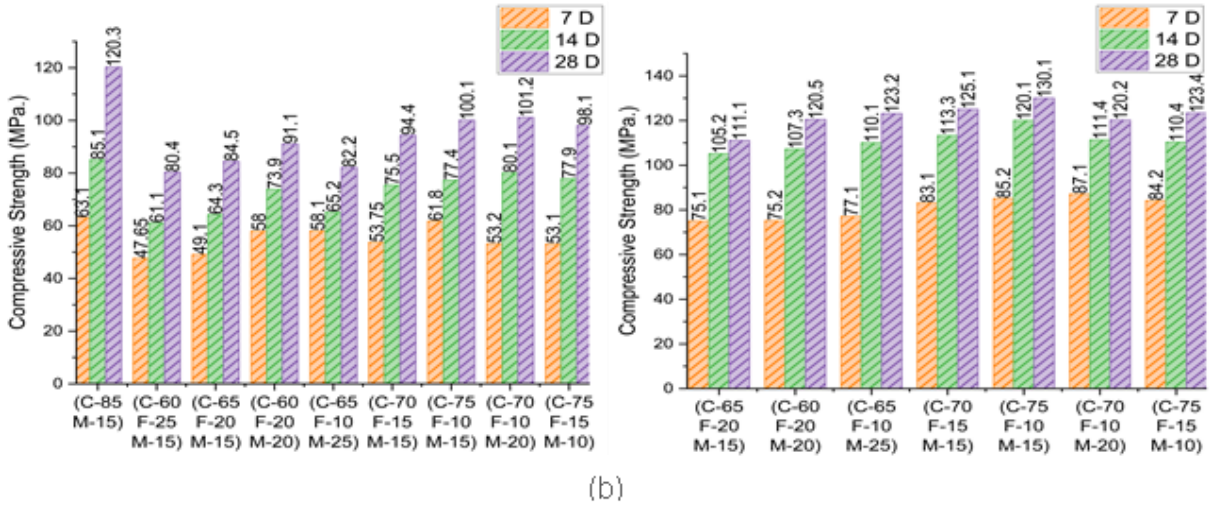

Figure 4. (a) slump flow results and (b) compressive strength results for various mixes

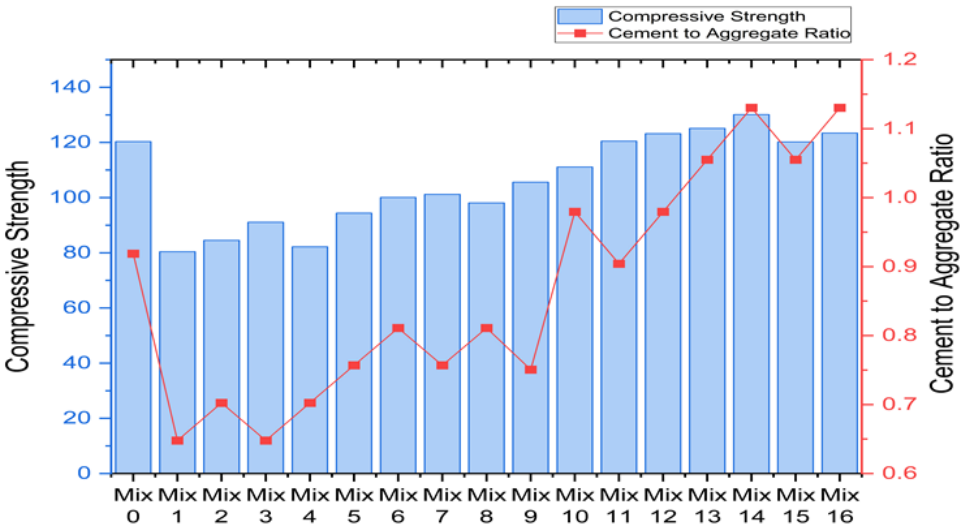

Figure 5. Compressive strength vs. cement to aggregate ratio

3.3 Flexural strength of UHPC

Figure 6 shows the flexural strengths of Mixes 0-8 and Mixes 9-16. An experimental study was conducted to observe the increase in the flexural strength when the silica content was increased from 15-25 %. There was a noticeable increase in flexural strength from Mix 5 to Mix 8 as the amount of cement increased. The flexural strength of Mixes 9-16 can be enhanced by increasing the cementitious concentration from 1200-1400 kg/m^3. The amalgamation of steel fibres significantly enhanced the overall strength of UHPC after a curing period of 28 d. The overall flexural strength of UHPC was observed to increase as a function of the percentage of steel fibres and binder content. Additionally, the augmentation of flexural strength correlated with higher silica contents and increased formation of C-S-H gel, as indicated by Laun et al. [28].

3.4 Indirect tensile strength of UHPC

Figure 7 displays the split tensile strengths of Mixes 0-8 and Mixes 9-16 after 14 and 28 d. According to the ASTM C1856 standard, the minimum split tensile strength should exceed 6 MPa. The split tensile strength of Mixes 1-7 increased from 11 MPa to 13 MPa with an increase

in the amount of cement and micro-silica. The post-cracking behaviour and ductility cannot be evaluated using a direct tensile test. Mixes 9-16 provided superior split tensile strength values compared with Mixes 0-8, mostly owing to the higher amount of cementitious material present. The incorporation of steel fibres significantly enhanced the tensile strength of UHPC after 14 and 28 d. Increasing the number of steel fibres and the binder content has been found to enhance the static tensile strength of UHPC. Research findings indicate that the incorporation of 1,5 % steel fibres leads to a notable improvement in tensile strength. However, additional investigations are required to assess the post-tensile behaviour through direct tensile strength testing, as suggested by studies conducted by Aimin et al. [37] and Ferdosian et al. [38].

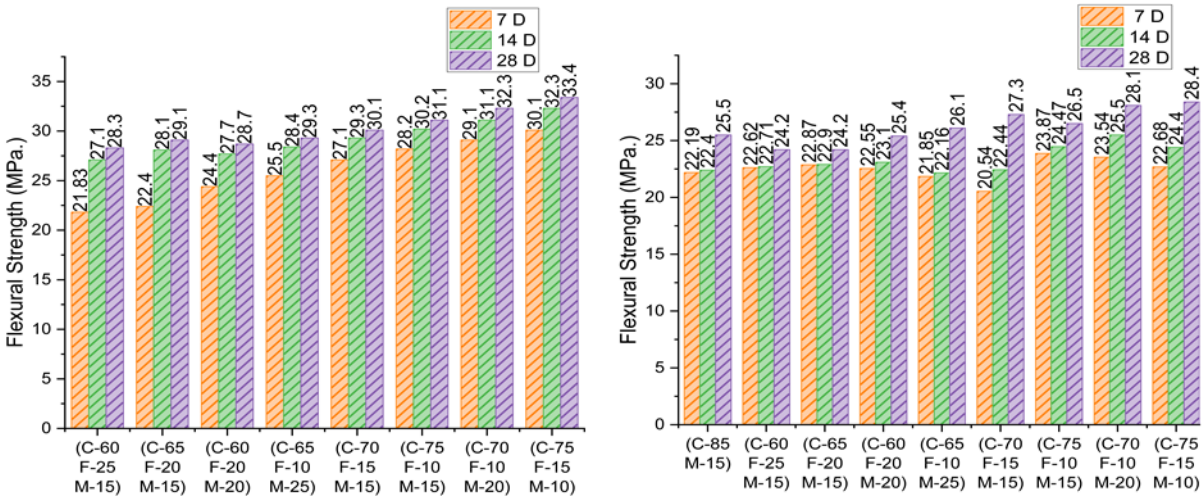

Figure 6. Flexural strength results

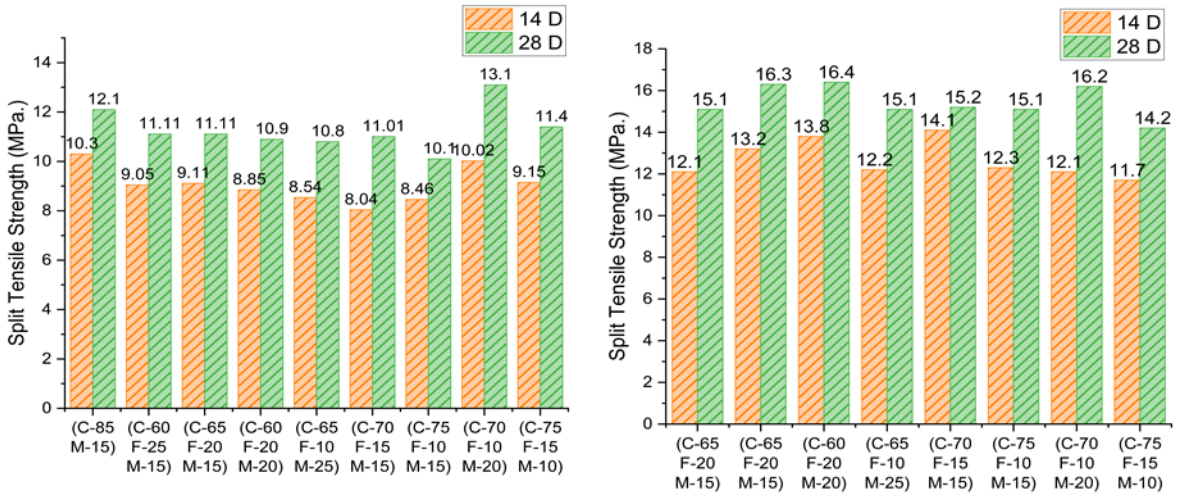

Figure 7. Split tensile strength for various mixes

3.5 Embodied CO_2 emissions of UHPC

Traditional UHPC typically contains cementitious concentrations ranging from 1200-1600 kg/m^3, resulting in elevated levels of CO_2 emissions. The integration of supplementary cementitious materials (SCMs) is advantageous in enhancing their sustainability.

To assess the embedded CO2 emissions, we calculated the lowest embodied CO_2 index (ECI) and unit cement strength index (CSI), which are represented by Eq. (4) and (5). The indices were employed to evaluate the collective impact of environmental factors and the mechanical characteristics of UHPC.

$$ECI = \frac{embodied\ CO_2\ (kg/m^3)}{\sigma(MPa)} \quad (4)$$

$$CSI = \frac{Compressive\ Strength\ (MPa)}{Cement\ Content\ (kg/m^3)} \quad (5)$$

The embedded CO_2 (e-CO_2) emissions considered for major processes include the raw material manufacturing, transportation, and curing phases of concrete. The total CO_2 was calculated by adding the e-CO_2 of the raw materials and the unit volume of concrete. Based on the available literature, the embodied CO_2 of various materials is listed in Table 5.

Table 5. Embodied CO_2 of various UHPC materials

Items	e-CO_2 per kg	References
cement	0,8300	[39]
fly ash	0,0090	[39]
micro silica	0,0000	[40]
fine sand	0,0010	[39]
high range water reducer (superplasticizer)	0,7200	[39]
shrinkage reducing admixture	0,0860	[39]
micro steel fibers	1,4875	[40]
water	0,0003	[41]

Table 6. Compressive strength, e-CO_2, ECI, and CSI index for various Mixes

Mix Design	Compressive Strength (MPa)	e-CO_2 (kg/m^3)	ECI (kg/MPa.m^3)	CSI (MPa.m^3/kg)
Mix 0 (C-85/M-15)	120,3	1044	8,68	0,12
Mix 1 (C-60/F-25/M-15)	80,4	795	9,89	0,11
Mix 2 (C-65/F-20/M-15)	84,5	845	10,00	0,11
Mix 3 (C-60/F-20/M-20)	91,1	795	8,73	0,13
Mix4 (C-65/F-10/M-25)	82,2	844	10,27	0,10
Mix 5 (C-70/F-15/M-15)	94,4	895	9,48	0,11
Mix 6 (C-70/F-10/ M-15)	100,1	945	9,44	0,11
Mix 7 (C-70/F-10 M-20)	101,2	895	8,84	0,12
Mix 8 (C-75/F-15/M-10)	98,1	946	9,64	0,11
Mix 9 (C-60/ F-25/ M-15)	105,6	893	8,46	0,13
Mix 10 (C-65/ F-20/ M-15)	111,1	951	8,56	0,12
Mix 11 (C-60/ F-20/ M-20)	120,5	893	7,41	0,14
Mix 12 (C-65/ F-10/ M-25)	123,2	949	7,70	0,14
Mix 13 (C-70/ F-15/ M-15)	125,1	1008	8,06	0,13
Mix 14 (C-75/ F-10/ M-15)	130,1	1066	8,19	0,12
Mix 15 (C-70/ F-10/ M-20)	120,2	1008	8,39	0,12
Mix 16 (C-75/ F-15/ M-10)	123,4	1066	8,64	0,12

In Table 6, we present the relationship between the compressive strength, embodied CO_2 (e-CO_2), ECI, and CSI for various UHPC mixes. Figure 8 illustrates the relationship between the compressive strength and e-CO_2 index. Our analysis reveals a distinct trend; as the compressive strength of UHPC increases, the ECI decreases. Moreover, our linear regression analysis highlights a significant relationship between the e-CO_2 index and compression strength, with an R^2 value of 0,7382. Consequently, variations in the e-CO_2 index were predictive of changes in compressive strength, affirming a tangible link between these two

variables. Notably, mixes 11 and 12 exhibited the lowest e-CO_2 values, despite possessing compressive strengths exceeding 120 MPa. In addition, the unit cement strength index was notably higher for mixes 11 and 12. These findings provide valuable insights into the interplay between the material composition, environmental impact, and structural performance of UHPC mixes. By identifying mixes with lower e-CO_2 values and higher compressive strengths, our findings on ECI and CSI facilitate decision-making in sustainable construction practices, aligning structural requirements with environmental considerations.

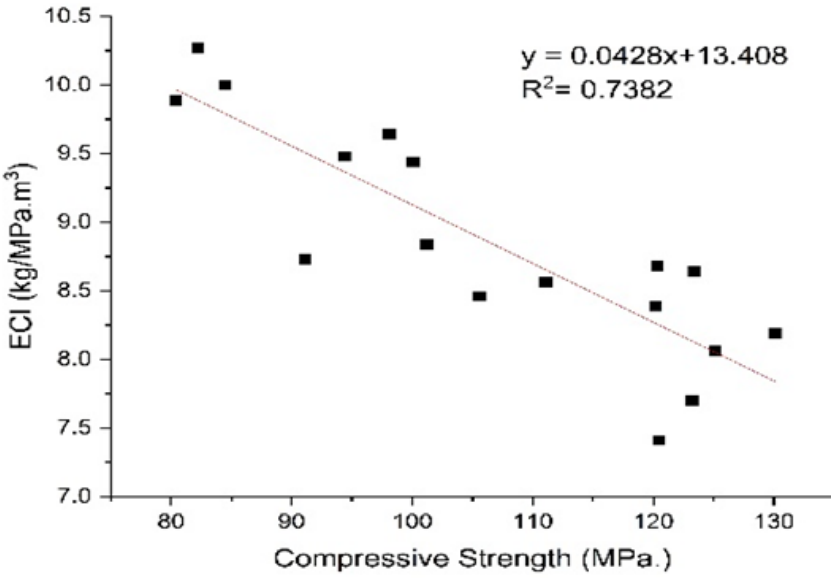

Figure 8. Plot of ECI (kg/MPa.m^3) vs. compressive strength (MPa)

4 Conclusions

This study investigated the production of UHPC using locally sourced materials. An experiment served as the foundation for this analysis by examining 17 different mix variations with varying binder concentrations and water-to-binder ratios. Mechanical parameters such as compressive, flexural, and split tensile strengths were evaluated in conjunction with slump flow data. The findings were as follows:

- The flow values increased with increasing binder content and ranged from 1200-1400 kg/m^3. All 17 mixes satisfied the flow parameters outlined in the ASTM C1856 standard [31] with the provided water-to-binder ratio.
- Initially, the fly-ash-based mixes exhibited lower compressive strengths compared with the control mix but later demonstrated improved mechanical strength. The compressive strengths of Mixes 9-16 increased with a higher binder concentration ranging from 1200-1400 kg/m^3, with Mixes 13 and 14 showing the highest replacement and compressive strengths.
- Steel fibres enhance flexural strength compared with ordinary concrete. As the binder content increased from Mixes 0-8 and Mixes 9-16, the flexural strength improved. Further iinvestigation is required to analyse the post-cracking behaviour, with Mixes 15 and 16 demonstrating the highest flexural strengths.
- The use of steel fibres influences the indirect tensile strength; Mixes 9–16 exhibited higher tensile strengths than Mixes 0-8. Mixes 11 and 15 exhibited the highest tensile strengths.
- The results indicate that replacing 15-20 % with micro-silica and 10-20 % with fly ash can enhance the compressive, flexural, and indirect tensile strengths. Strengthening is attributed to the refinement of the pore structure and an increase in the pozzolanic

reactivity of micro-silica. The optimal replacement ratios for mechanical properties were identified as those of C75/F10/M15 and C70/F10/M20.

- Regarding the low CO2 emissions and carbon footprints, C-60/ F-20/ M-20 and C-65/ F-10/ M-25 were more economical.

Acknowledgments

The authors would like to express gratitude to Nirma University, Ahmedabad, Gujarat, India, for providing infrastructure and facilities necessary for conducting the testing and experimentation work.

References

[1] US Department of Transportation, Federal Highway Administration. FHWA Publication No.: FHWA-HRT-14-041: Splice Length of Prestressing Strand in Field-Cast Ultra-High Performance Concrete Connections. Accessed: February 17, 2024. Available at: https://rosap.ntl.bts.gov/view/dot/35815/dot_35815_DS1.pdf

[2] Sadrekarimi, A. Development of a Light Weight Reactive Powder Concrete. *Journal of Advanced Concrete Technology*, 2004, 2 (3), pp. 409-417. https://doi.org/10.3151/jact.2.409

[3] Richard, P.; Cheyrezy, M. Composition of reactive powder concretes. *Cement and Concrete Research*, 1995, 25 (7), pp. 1501-1511. https://doi.org/10.1016/0008-8846(95)00144-2

[4] Azmee, N. M.; Shafiq, N. Ultra-high performance concrete: From fundamental to applications. *Case Studies in Construction Materials*, 2018, 9, e00197. https://doi.org/10.1016/j.cscm.2018.e00197

[5] Birchall, J. D.; Howard, A. J.; Kendall, K. Flexural strength and porosity of cements. *Nature*, 1981, 289, pp. 388-390. https://doi.org/10.1038/289388a0

[6] Rossi, P.; Arca, A.; Parant, E.; Fakhri, P. Bending and compressive behaviours of a new cement composite. *Cement and Concrete Research*, 2005, 35 (1), pp. 27-33. https://doi.org/10.1016/j.cemconres.2004.05.043

[7] Blais P. Y.; Couture, M. Precast, Prestressed Pedestrian Bridge World's First Reactive Powder Concrete Structure. *PCI Journal*, 1999, 44 (5), pp. 60-71. https://doi.org/10.15554/PCIJ.09011999.60.71

[8] Yalçınkaya, Ç.; Çopuroğlu, O. Hydration heat, strength and microstructure characteristics of UHPC containing blast furnace slag. *Journal of Building Engineering*, 2021, 34, 101915. https://doi.org/10.1016/j.jobe.2020.101915

[9] Yu, R. et al. Sustainable development of Ultra-High Performance Fibre Reinforced Concrete (UHPFRC): Towards to an optimized concrete matrix and efficient fibre application. *Journal of Cleaner Production*, 2017, 162, pp. 220-233. https://doi.org/10.1016/j.jclepro.2017.06.017

[10] Tafraoui, A.; Escadeillas, G.; Lebaili, S.; Vidal, T. Metakaolin in the formulation of UHPC. *Construction and Building Materials*, 2009, 23 (2), pp. 669-674. https://doi.org/10.1016/j.conbuildmat.2008.02.018

[11] Amin, M.; Zeyad, A. M.; Tayeh, B. A.; Saad Agwa, I. Effect of ferrosilicon and silica fume on mechanical, durability, and microstructure characteristics of ultra high-performance concrete. *Construction and Building Materials*, 2022, 320, 126233. https://doi.org/10.1016/j.conbuildmat.2021.126233

[12] Van Tuan, N. et al. The study of using rice husk ash to produce ultra high performance concrete. *Construction and Building Materials*, 2011, 25 (4), pp. 2030-2035. https://doi.org/10.1016/j.conbuildmat.2010.11.046

[13] Alharbi, Y. R.; Abadel, A. A.; Mayhoub, O. A.; Kohail, M. Effect of using available metakaolin and nano materials on the behavior of reactive powder concrete. *Construction and Building Materials*, 2021, 269, 121344. https://doi.org/10.1016/j.conbuildmat.2020.121344

[14] Ha, N. S. et al. Effect of grounded blast furnace slag and rice husk ash on performance of ultra-high-performance concrete (UHPC) subjected to impact loading. *Construction and Building Materials*, 2022, 329, 127213. https://doi.org/10.1016/j.conbuildmat.2022.127213

[15] Wille, K.; Naaman, A. E.; El-Tawil, S.; Parra-Montesinos, G. J. Ultra-high performance concrete and fiber reinforced concrete: Achieving strength and ductility without heat curing. *Materials and Structures*, 2012, 45, pp. 309-324. https://doi.org/10.1617/s11527-011-9767-0

[16] Shen, P. et al. The effect of curing regimes on the mechanical properties, nano-mechanical properties and microstructure of ultra-high performance concrete. *Cement and Concrete Research*, 2019, 118, pp. 1-13. https://doi.org/10.1016/j.cemconres.2019.01.004

[17] Zhuang, W.; Li, S.; Yu, Q. The effect of supplementary cementitious material systems on dynamic compressive properties of ultra-high performance concrete paste. *Construction and Building Materials*, 2022, 321, 126361. https://doi.org/10.1016/j.conbuildmat.2022.126361

[18] Abdellatief, M. e al. Development of ultra-high-performance concrete with low environmental impact integrated with metakaolin and industrial wastes. *Case Studies in Construction Materials*, 2023, 18, e01724. https://doi.org/10.1016/j.cscm.2022.e01724

[19] Shi, C. et al. A review on ultra high performance concrete: Part I. Raw materials and mixture design. *Construction and Building Materials*, 2015, 101 (Part 1), pp. 741-751. https://doi.org/10.1016/j.conbuildmat.2015.10.088

[20] Burroughs, J. F.; Weiss, J.; Haddock, J. E. Influence of high volumes of silica fume on the rheological behavior of oil well cement pastes. *Construction and Building Materials*, 2019, 203, pp. 401-407. https://doi.org/10.1016/j.conbuildmat.2019.01.027

[21] Dong, P. S. et al. Compressive strength development of high-volume fly ash ultra-high-performance concrete under heat curing condition with time. *Applied Sciences*, 2020, 10 (20), 7107. https://doi.org/10.3390/app10207107

[22] Singh, B. et al. Influence of the Packing Density of Fine Particles in Ternary, Quaternary and Quinary Blends on High Performance Concrete. In: *3rd International Conference on Innovative Technologies for Clean and Sustainable Development. RILEM Bookseries*, Ashish, D. K.; de Brito, J.; Sharma S. K. (eds.). February 19-21, 2020, Chandigarh, India, Springer; 2021, 29, pp. 465-482. https://doi.org/10.1007/978-3-030-51485-3_31

[23] Jing, R.; Liu, Y.; Yan, P. Uncovering the effect of fly ash cenospheres on the macroscopic properties and microstructure of ultra high-performance concrete (UHPC). *Construction and Building Materials*, 2021, 286, 122977. https://doi.org/10.1016/j.conbuildmat.2021.122977

[24] Li, H. et al. Preparation of water-quenched manganese slag and fly ash ultrafine mineral admixture and its application in UHPC. *International Journal of Low-Carbon Technologies*, 2023, 18, pp. 628-636. https://doi.org/10.1093/ijlct/ctac143

[25] Hakeem, I. Y.; Althoey, F.; Hosen, A. Mechanical and durability performance of ultra-high-performance concrete incorporating SCMs. *Construction and Building Materials*, 2022, 359, 129430. https://doi.org/10.1016/j.conbuildmat.2022.129430

[26] Kareem, R. et al. Developing Sustainable Ultra-High-Performance Concrete. *ACI Materials Journal*, 2022, 119 (3), pp. 127-136. https://doi.org/10.14359/51734607

[27] Ahmad, S. et al. Durability and Mechanical Aspects of UHPC Incorporating Fly Ash and Natural Pozzolan. *Arabian Journal for Science and Engineering*, 2023, 49, pp. 5255-5266. https://doi.org/10.1007/s13369-023-08416-1

[28] Luan, C. et al., The effects of calcium content of fly ash on hydration and microstructure of ultra-high performance concrete (UHPC). *Journal of Cleaner Production*, 2023, 415, 137735. https://doi.org/10.1016/j.jclepro.2023.137735

[29] Ghanim, A. A. J. et al. Effect of modified nano-titanium and fly ash on ultra-high-performance concrete properties. *Structural Concrete*, 2023, 24 (5), pp. 6815-6832. https://doi.org/10.1002/suco.202300053
[30] Bureau of Indian Standards. IS: 12269-1987. *Specification for 53 grade ordinary Portland cement*. New Delhi: IS; 1988.
[31] ASTM International. C1856/C1856M Standard Practice for Fabricating and Testing Specimens of Ultra-High Performance Concrete. Accessed: February 17, 2024. Available at: https://www.astm.org/c1856_c1856m-17.html
[32] Bureau of Indian Standards. IS 516: 1959. *Method of Tests for Strength of Concrete*. New Delhi: IS; 1959.
[33] Bureau of Indian Standards. IS: 4031 (Part 8) 1988. *Methods of physical tests for hydraulic cement, Part 8: Determination of transverse and compressive strength of plastic mortar using prism*. New Delhi: IS; 1988.
[34] ASTM International. C143/C143M-09 standard test method for Slump of Hydraulic-Cement Concrete. Accessed: February 17, 2024. Available at: https://www.astm.org/c0143_c0143m-09.html
[35] Ge, W, et al. Sustainable ultra-high performance concrete with incorporating mineral admixtures: Workability, mechanical property and durability under freeze-thaw cycles. *Case Studies in Construction Materials*, 2023, 19, e02345. https://doi.org/10.1016/j.cscm.2023.e02345
[36] Mashaly, A. A.; Mahdy, M. G.; Elemam, W. E. Optimal design and characteristics of sustainable eco-friendly ultra-high-performance concrete. *Innovative Infrastructure Solutions*, 2023, 8, 326. https://doi.org/10.1007/s41062-023-01277-5
[37] Zhang, A. et al. Static and dynamic tensile properties of ultra-high performance concrete (UHPC) reinforced with hybrid sisal fibers. *Construction and Building Materials*, 2024, 411, 134492. https://doi.org/10.1016/j.conbuildmat.2023.134492
[38] Ferdosian. I.; Camões, A. Mechanical performance and post-cracking behavior of self-compacting steel-fiber reinforced eco-efficient ultra-high performance concrete. *Cement and Concrete Composites*, 2021, 121, 104050. https://doi.org/10.1016/j.cemconcomp.2021.104050
[39] Long, G.; Gao, Y.; Xie, Y. Designing more sustainable and greener self-compacting concrete. *Construction and Building Materials*, 2015, 84, pp. 301-306. https://doi.org/10.1016/j.conbuildmat.2015.02.072
[40] Chiaia, B. et al. Eco-mechanical index for structural concrete. *Construction and Building Materials,* 2014, 67 (Part C), pp. 386-392. https://doi.org/10.1016/j.conbuildmat.2013.12.090
[41] Amran, M. et al. Sustainable development of eco-friendly ultra-high performance concrete (UHPC): Cost, carbon emission, and structural ductility. *Construction and Building Materials*, 2023, 398, 132477. https://doi.org/10.1016/j.conbuildmat.2023.132477